Case Studies in Thermal Engineering 28 (2021) 101663

Contents lists available at ScienceDirect

Case Studies in Thermal Engineering

journal homepage: www.elsevier.com/locate/csite

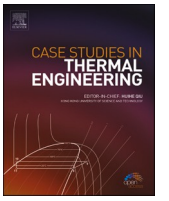

Applicability of an organic Rankine cycle for a liquid desiccant-assisted dedicated outdoor air system in apartments

Beom-Jun Kim, Hye-Won Dong, Jae-Weon Jeong *

Department of Architectural Engineering, College of Engineering, Hanyang University, Seoul, 04763, South Korea

ARTICLE INFO

Keywords:
Organic Rankine cycle
Waste heat
Heat-driven system
Central ventilation system
Apartments

ABSTRACT

This study investigates the dehumidification and energy performance of central ventilation systems based on a liquid desiccant-assisted dedicated outdoor air system applied to an apartment residential building. This heat-driven central ventilation system should receive heat energy because of regenerating the liquid desiccant. An organic Rankine cycle (ORC) consists of the central ventilation system proposed in this study to provide heat to the regeneration of the desiccant solution. The overall configuration of the ventilation system consists of three main devices, a liquid type of desiccant system, an evaporative cooler driven indirectly to utilize free cooling energy, and the electric heating coil to supply the process air at a neutral temperature condition. The size of the ORC is determined to provide the base electricity demand of community facilities in the apartment selected in this study. The evaluation of the size and energy performance is conducted through a detailed simulation. The results of the energy simulation are compared with heat-driven desiccant wheel and conventional energy recovery ventilation systems. The proposed system demonstrates 4%–24% lower annual primary energy consumption than two existing ventilation systems. This result can be expected that the proposed liquid desiccant-based central ventilation system incorporating ORC is possible to contribute to the achievement of the zero-energy building by using both electricity and heat energy.

1. Introduction

The introduction of a combined heat and power (CHP) system applied to residential buildings contributes greatly to providing electricity and heat energy for the certification of zero energy buildings. Meanwhile, an organic Rankine cycle (ORC) has gained significant attention as the CHP system that produces electricity and heat energy (e.g., solar thermal, geothermal, and various wasted heat sources). Previous researchers performed thermodynamic analysis on various heat sources and showed that the ORC has good energy efficiency when combined with low heat sources [1–4]. The electricity produced in the ORC is available in a variety of places. Also, the use of ORC as an electric power source for operating air-conditioning systems has been conducted based on the vapor compression heat pump system. Wang et al. [5,6] introduced the ORC used for operating the vapor compression cycle, while the heat from the ORC was released to the surroundings. Their system presented 5 kW of a nominal cooling capacity. Bu et al. studied an ORC-powered vapor compression air-conditioning system considering a geothermal heat source and derived a thermodynamic model [7].

* Corresponding author.
E-mail address: jjwarc@hanyang.ac.kr (J.-W. Jeong).

https://doi.org/10.1016/j.csite.2021.101663
Received 24 May 2021; Received in revised form 11 November 2021; Accepted 18 November 2021

Available online 19 November 2021

Nomenclature

A	room area [m^2]
a	area-to-volume ratio of media surface [m^2/m^3]
BEC	boiler efficiency curve [−]
C	thermal capacitance [kW]
c	specific heat [kJ/kg-°C]
DBT	dry bulb temperature [−]
DFR	driving force ratio [−]
EIR	energy input ratio [−]
ff	flow fraction [−]
GFR	flow rate of gas [kg/s]
h	enthalpy [kJ/kg]
HR	humidity ratio [−]
LE	latent effectiveness [−]
LFR	flow rate of liquid[kg/s]
$\dot{m}$	mass flow rate [kg/s]
N	number [−]
ΔP	pressure drop difference [kPa]
$\dot{Q}$	thermal energy [kJ/s]
RTF	run-time fraction [−]
SE	sensible effectiveness [−]
T	temperature [°C]
V	velocity [m/s]
$\dot{V}$	volume flow rate [m^3/s]
$\dot{W}$	power [kW]
Zh	height of packing media [m]
π	ratio of a vapor pressure difference between water to solution to the water vapor pressure
γ_L	surface tension of the desiccant solution based wetting characteristics
γ_c	critical surface tension based wettability of the packing media

Greek Symbols

α	relative humidity effectiveness of the desiccant wheel [−]
β	enthalpy humidity effectiveness of the desiccant wheel [−]
ε	effectiveness [−]
η	efficiency [−]
ω	humidity ratio [kg/kg]

Subscripts

a	air
ab	absorber
aux	auxiliary
bed	bedchamber
chiller	chiller
cd	condenser of the ORC
CWS	chilled water supply
DBT	dry-bulb temperature
dehum	dehumidification
district	district heat source
DX	direct expansion
e	equilibrium
ep	evaporator of the ORC
EW	enthalpy wheel
exh	exhaust air
fg	vaporization
h	enthalpy
heater	gas-fired heater
HX	heat exchanger
i	inlet
lat	latent

net	net power
o	outlet
outa	outdoor air
occu	occupants
orc	organic Rankine cycle
pres	pressure
pro	process air
ra	room or zone return air
ref	reference
reg	regenerator
req	required humidity ratio
RH	relative humidity
sa	supply air
sen	sensible
set	setpoint
sol	liquid desiccant solution
SW	sensible wheel
tot	total
tur	turbine
unit	each household unit
v	velocity

Abbreviations

DW	desiccant wheel
DX-coil	direct expansion coil
EA	exhaust air
EW	enthalpy wheel
HX	heat exchanger
LD	liquid desiccant
OA	outdoor air
ORC	organic Rankine cycle
RA	room or zone return air
SA	supply air
SW	sensible wheel

On the other hand, when the ORC is considered as the CHP system for building applications, heat energy should be used in conjunction with heat-driven systems to achieve the most effective energy savings. Because the heat energy of ORC cannot be used in the industry or linked to other CHP systems for further electricity generation because of its low temperature showing just 40–60 °C. Most of utilizing ORC systems depend solely on generating electricity, and how to use heat from ORC was not deeply considered. The heat-driven systems would be sufficient for the ORC to utilize heat and electric power in the building simultaneously. However, most heat-driven air-conditioning systems such as absorption and adsorption cooling system need to receive high-temperature heat [8], which cannot be supplied by the ORC generating heat and power from the heat source of the low temperature available near a building.

A dehumidification system of the ventilation system can be a key solution in residential buildings or apartments, as heat energy is essential for the regeneration of the dehumidifier. The ventilation system, specially dedicated outdoor air system (DOAS) is a decoupled system to supply the ventilation air for indoor occupants and remove latent load—outdoor air dehumidification—of the target zone. To process the outdoor air as a dry condition in humid weather, various dehumidifying components can be applied to the DOAS (e.g., condensation dehumidification, solid desiccant, and liquid desiccant). Among them, liquid desiccant requires the lowest temperature condition required to regenerate the desiccant solution at 40 °C–60 °C. Therefore, the liquid desiccant solution can be regenerated by receiving sufficient heat from a relatively low heat source such as PVT, district heat. And also it is possible to dehumidify by obtaining free energy when dehumidifying the hot and humid ventilation air in summer.

Recently, liquid desiccant (LD) dehumidification-assisted air-conditioning systems [7,9–12] have gained significant attention owing to their desirable characteristics considering energy saving and indoor environmental control, while they need to receive relatively low-temperature heat (e.g., 50–70 °C) for regenerating weakened desiccant solutions [8,13–16]. This point is also applicable when heat is supplied to the liquid desiccant system from ORC. The ORC can supply heat to the regeneration of the desiccant solution after producing electricity from low-grade heat sources. In particular, the ORC can be expected to supply continuous heat energy compared to using PVT which may not be constant to supply heat. Despite these advantages, only a limited number of studies exist for this solution. Jradi and Riffat [17] evaluated ORC integrated with an LD-assisted cooling system operated by a biomass fuel. However, they used biomass fuel as the heat source for both ORC and LD regeneration independently, and the heat energy released from the ORC was exhausted in the atmosphere.

Consequently, the ORC can produce beneficial efficiency when used with LD because it can fully utilize the low heat source. Additionally, because such low-grade heat sources are commonly available in any building, the ORC can be easily considered for residential buildings, including high-rise apartments. However, not enough research has been done on the LD systems incorporating ORC. Only Dong et al. [18] demonstrated that sufficient energy-saving potential can be expected in buildings by applying the ORC to an air-conditioning system with LD utilizing from the district heat source for the ORC, but more follow-up studies are required to compare the applicability of the heat-driven ventilation systems [19].

To develop the previous research, the applicability analysis is conducted for the ORC-based heat-driven central ventilation system proposed in this study for the apartment building. The proposed ventilation system consists of three main parts, an LD dehumidifier, an indirect evaporative cooler to utilize free cooling energy, and the electric heating coil to supply the process air at a neutral temperature. To succeed in the applicability analysis of the proposed system for the apartment building, two existing ventilation systems are compared with the system proposed in this research to evaluate that how much energy can be saved. The one is a desiccant wheel-based ventilation system, and the other is an enthalpy wheel and cooling coil-based ventilation system. In addition, the CHP systems such as ORC must make sizing decisions based on either heat or electricity demand [20,21]. In this research, the ORC is applied to a model apartment building to accommodate the base electrical demand of community facilities, and the gained heat is utilized for the heat up the weak solution for the regeneration process. The analysis of the energy benefit is initially conducted for the design day with the most humid outdoor air condition (i.e., peak dehumidification load). All the energy performance and the COP of the systems are estimated via an annual energy simulation in detail. The researchers who read this paper can get some ideas as follows: (1) how heat-driven CHP systems such as ORC can be used as desiccant-based central ventilation systems; and (2) where the heat and electricity produced by ORC can be utilized.

2. Central ventilation systems

2.1. Proposed system

The proposed system is a ventilation system consisting of an LD dehumidifier, an evaporative cooler that can indirectly cool the process air, and an electric reheating coil (Fig. 1). The main system is designed as a dedicated outdoor system (DOAS) that uses 100% of outdoor air to ventilate the room and remove the latent heat load of the zone. The process air is the minimum required ventilation air meeting the local ventilation code [22]. In climates with frequent hot and humid conditions, the LD dehumidifier should operate to dehumidify the introduced humid air. A strong desiccant solution (e.g., 30%–40% lithium chloride solution) was sprayed into the absorber, and the humidity of the introduced air is absorbed by the strong desiccant. The liquid desiccant has to be cooled to approximately 20–25 °C before it enters the absorber because dehumidification is an exothermic process, and this can enhance the dehumidification efficiency [15]. The solution after the dehumidification process should be heated to approximately 55–60 °C [23] and then supplied onto the packed bed of the regenerator as a spray form. Scavenger air (e.g., outdoor air) flowing through a regenerator takes away moisture from the heated desiccant solution. The released heat from the condenser of the ORC is reclaimed as a heat source for the regenerator described in Fig. 1.

The dehumidified process air gets cool effect by the indirect evaporative cooler for the satisfaction of the target temperature

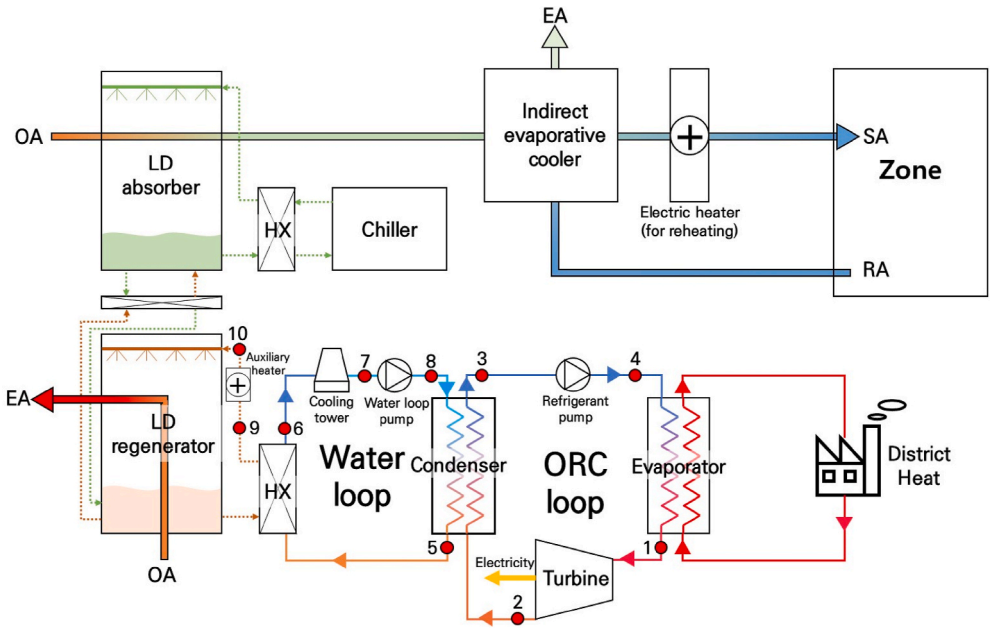

Fig. 1. Schematic of the ORC-based central ventilation system consisted of LD and indirect evaporative cooler.

condition (e.g., neutral temperature); otherwise, it does not operate. The electric reheating coil is activated when the cold supply air condition is detected to set the target temperature. Also, when the dry and cold outdoor air condition is occurred, the electric reheating coil is activated for the cold process air to meet the neutral temperature. The remaining thermal load of the zone is met by the indoor air-conditioning system (i.e., parallel system) installed in each apartment household unit (e.g., room air conditioner).

2.1.1. Organic Rankine cycle

In Fig. 1, the liquid-phase refrigerant is vaporized by absorbing heat from the heat source (e.g., district heat at 80–130 °C) in the evaporator (at point 1) [24]. The ORC turbine receives the hot refrigerant gas at high pressure and generates electric power (at point 2). The organic refrigerant with high-temperature inflows to the condenser and the heat is transferred with the water loop (at points 3 and 5). The water loop is consisting of two heat sinks; the one is a heat exchanger (HX) for the solution that heats the weak desiccant to the regeneration temperature (e.g., 55–60 °C) before it enters the regenerator (at point 6), and the other is a cooling tower to ensure the condensing performance by cooling the water in the water loop because the condenser should release the heat well (at point 7). The pumps of the ORC loop and water loop just carry the fluid in each loop. When the fluids pass through the pump, there m may be temperature change due to slight friction. But it is assumed to be neglected in this paper and there is no change of the temperature (at the point 4 and 8). Eq. 1 through 5 are used to determine the ORC performance based on the mass flow rate ($\dot{m}$), enthalpy (h), and temperature (T) of each working fluid at each state point defined in Fig. 1.

$$\dot{Q}_{evap} = \dot{Q}_{district} = \dot{m}_{orc}(h_1 - h_4) \tag{1}$$

$$\dot{W}_{tur} = \eta_{tur}\dot{m}_{orc}(h_1 - h_{2s}) \tag{2}$$

$$\dot{Q}_{cond} = \dot{m}_{orc}(h_2 - h_3) \tag{3}$$

$$\dot{W}_{pump} = \frac{\dot{m}_{orc}(h_{4s} - h_3)}{\eta_{pump}} \tag{4}$$

$$\dot{W}_{net} = \dot{W}_{tur} - \dot{W}_{pump} \tag{5}$$

The amount of heat transferred from the condenser of the ORC to the weak desiccant solution for regeneration ($\dot{Q}_{reg.actual}$) is determined by using Eq. 6 through 12.

$$\dot{Q}_{water} = \eta_{cond}\dot{Q}_{cond} \tag{6}$$

$$C_{water} = \dot{m}_{water}c_{p.water} \tag{7}$$

$$T_5 = T_8 + \frac{\dot{Q}_{water}}{C_{water}} \tag{8}$$

$$\dot{Q}_{reg.max} = \dot{m}_{water}c_{p.water}(T_5 - T_9) \cdot \left(if\ \dot{m}_{water}c_{p.water} \le \dot{m}_{sol}c_{p.sol}\right) \tag{9}$$

$$\dot{Q}_{reg.max} = \dot{m}_{sol}c_{p.sol}(T_5 - T_9) \cdot \left(if\ \dot{m}_{water}c_{p.water} > \dot{m}_{sol}c_{p.sol}\right) \tag{10}$$

$$\dot{Q}_{reg.actual} = \eta_{sol.heat.HX}\dot{Q}_{reg.max} \tag{11}$$

$$T_6 = T_5 - \frac{\dot{Q}_{reg.actual}}{\dot{m}_{water}c_{p.water}} \tag{12}$$

If more heat energy should need to heat the weak solution, the electric auxiliary heater is activated (at point 9 and 10). The target temperature condition of the solution was set to 60 °C. The amount of auxiliary heat was determined by Eqs. (13) and (14).

$$T_{10} = T_9 + \frac{\dot{Q}_{reg.actual}}{\dot{m}_{sol}c_{p.sol}} \tag{13}$$

$$\dot{Q}_{sol.aux.heating} = \dot{m}_{sol}c_{p.sol}\left(60 - T_{sol.reg.i}\right)(if \cdot \mathrm{T}_{10} < 60^{\circ}C) \tag{14}$$

The determination of the organic refrigerant for selecting the working fluid is an important process to operate the ORC. In the previous studies, the selection of organic refrigerant for the proposed system has been discussed [25,26]. Dong and Jeong [27] suggested Novec649 as the organic refrigerant for the ORC with the district heat source. According to previous studies, Novec649 is suitable for supplying regeneration heat to LD from a low-grade heat source (e.g., district heat) [27,28]. A pinch point was set to be 5 °C, which is typically considered in condenser design. The evaporation and condensation temperatures of the cycle are determined by keeping the pinch point of the evaporator and condenser constant. It was assumed that the state of the outlet side evaporator was

saturated steam and the state of the outlet side condenser was a saturated liquid. The mass flow rate of the water loop was assumed to be constant at 1.5 kg/s to constantly transfer the heat of the cycle to the regeneration unit. The pressure drop in the heat exchanger was neglected. The heat-supplying district heating temperature is set to 120 °C, and the temperature of the solution after dehumidification is set to 40 °C in the LD system. Physical design values, such as the turbine and pump efficiencies, effectiveness values of all heat exchanges, and the condensing water flow rate in the water loop are summarized in Table 1 [28,29].

It was assumed that the capacity of the ORC should accommodate the electricity demand of the community facilities within the apartment building such as elevators, the lighting in parking lots and corridors, and community centers. The heat released from the ORC after the power generation process was reclaimed to be used as the regeneration heat of the weak desiccant solution.

2.2. Reference systems

To evaluate the energy performance of the proposed system for the apartment building, two existing ventilation systems were suggested in Fig. 2. The one is desiccant wheel (DW)-based ventilation system shown in Fig. 2(a) to compare that which type of desiccant system has better energy performance in the same heat-driven ventilation system, and the other is enthalpy wheel (EW) and cooling coil-based ventilation system described in Fig. 2(b) to compare whether the proposed system has superior energy performance than the basic DOAS configuration. These systems are set as DOAS that uses 100% of outdoor air to ventilate the room and remove the latent heat load of the zone as same as the proposed system.

(1) Case 1

The reference case 1 system using a DW consists of a sensible wheel (SW), a direct-expansion cooling coil (DX-coil), an electric reheating coil, and an air heater driven by gas for regenerating the DW (Fig. 2(a)) [30]. The ambient air introduced to the system is dehumidified by the DW initially, wherein moisture is absorbed by the solid desiccant coated on a wheel matrix. The saturated DW is regenerated by the hot return air from the zone, which is heated by the gas-fired air heater to 80–90 °C for regeneration [31,32]. As shown in Fig. 2, the utilization of the heat from the ORC was conducted to pre-heat the return air before the gas-fired air heater. The capacity and operating conditions of the ORC integrated with reference case 1 are identical to those of the ORC applied to the proposed system.

Meanwhile, the dehumidified air after the DW becomes significantly high-temperature condition compared with the supply air set by neutral temperature; therefore, the SW is activated to cool the hot and dry process air by releasing excessive heat to the exhausting room airflow from the indoor unit. The SW also preheats the exhaust air by receiving the heat from the process air to save energy for regeneration. Then, the supply air meets the set condition by the DX-coil. The SW reduces both DX-coil and gas-fired regeneration air heater loads.

The DW should be inactivated because of the season of dry air condition (i.e., dehumidification is not required), while the SW and electric reheating coil would be used to set the neutral condition of the supply air.

(2) Case 2

The reference case 2 (Fig. 2(b)) is also a conventional dedicated outdoor air ventilation system [33]. The enthalpy of the outdoor air is initially exchanged through an EW. The introduced air is dehumidified and cooled after the EW. SW, a DX-coil, and an electric reheating coil. If the pre-conditioned process air does not satisfy the target humidity condition (e.g., 0.0097 kg/kg), additional dehumidification is occurred in the DX-coil by condensation of the process air. If the over-cooling occurs in the leaving air from the DX-coil and the process air should heat to meet the supply condition, the SW and electric coil reheat the process air.

3. Simulation overview

3.1. Model apartment building

A thirty-story apartment building was selected for the model of building thermal load served by three different centralized ventilation systems. The introduced outdoor air entering the ventilation system was supplied to each floor unit. The minimum ventilation rate required for each unit was determined using Eq. (15) [34]. The latent heat generated in each unit and the required humidity ratio of the supply air were also determined by follows (Eqs. (16) and (17) [35]):

Table 1
Physical design values of the ORC and water loop.

Design parameters	Value	Properties	Value
Refrigerant	Novec649	Boiling point	49 ° C
Evaporator pressure	500 kPa	Molecular weight	316 g/mol
Evaporator temperature	105 ° C	Critical point	169 MPa
Condenser pressure	150 kPa	Heat of vaporization	1.88 kJ/kg
Condenser temperature	60 ° C	Liquid density	1600 kg/m^3
Turbine efficiency	0.75	Specific heat	1.10 kJ/kgK
Pump efficiency	0.6	Thermal conductivity	0.059 W/mK
Heat exchanger efficiency	0.8	ODP	0
Water loop mass flow rate	1.5 kg/s	GWP	1

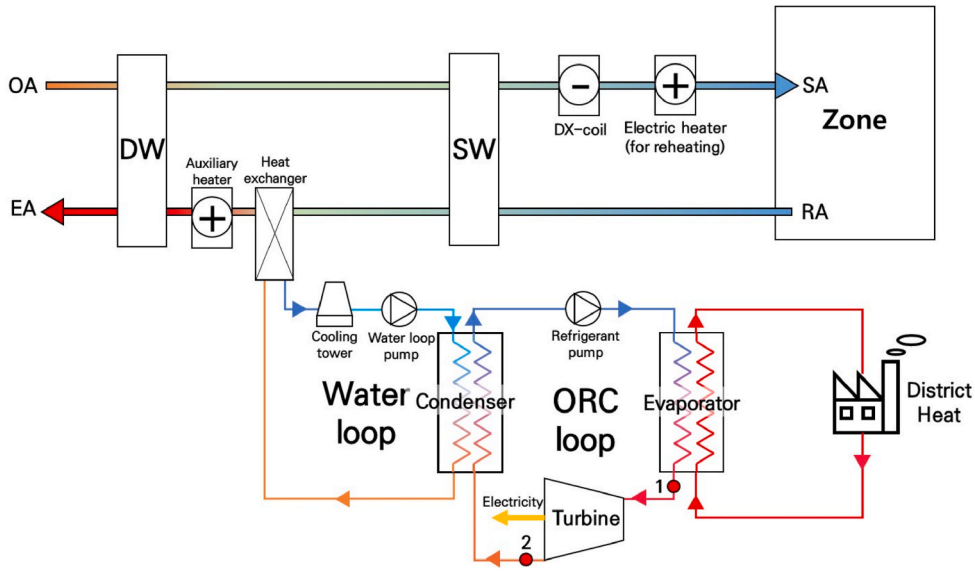

(a) Reference system consisted of the DW and SW with ORC for desiccant regeneration.

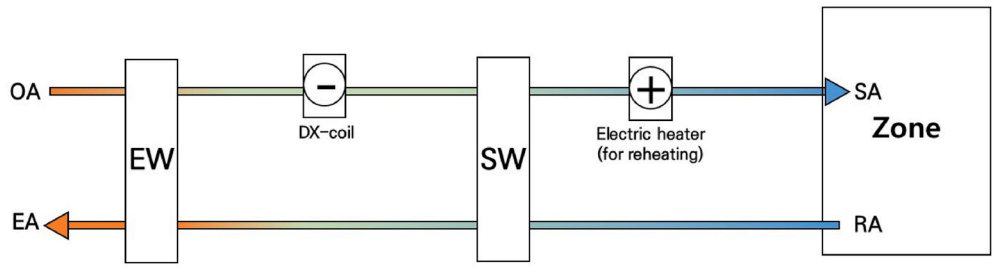

(b) Reference system consisted of the EW and SW.

Fig. 2. Schematic of reference system cases.

$$\dot{V}_{tot} = 0.15A_{unit} + 3.5(N_{bed} + 1) \tag{15}$$

$$\dot{Q}_{lat} = 20 + 0.22A_{unit} + 12N_{occu} \tag{16}$$

$$\omega_{req} = \omega_{ra} - \left(\frac{Q_{lat}}{3V_{tot}}\right) \tag{17}$$

An hourly thermal-load profile that should be met by each system case in the model apartment building was generated using calculation software for commercial building thermal loads [36]. Each floor had four residential units (Fig. 3). The height of the floor was 3 m. Further detailed information on the selected apartment building is presented in Table 2.

3.2. ORC capacity

Determining the sizing of the CHP system is not only important but also very difficult. The thermal and electricity demands of the building change from moment to moment throughout the year. Hence, when determining the capacity of the ORC, which energy to target will affect the size and operation of the ORC. In this study, the ORC capacity was determined to meet the demand for electricity for the community facilities within the model apartment building. The common electricity of the apartment building includes a parking lot, elevator, corridors, and community facilities. These facilities are suitable for ORC capacity calculation targets because they show a constant demand throughout the year. According to an existing study [38], apartment buildings similar to the model building consume 9.07 kWh/m^2-yr of electricity in community facilities. For the model apartment building, the total community area is 13,624 m^2, which indicates that the annual electricity demand for the community facilities of the model building would be 123.6 MWh/yr. If this annual electric demand is distributed uniformly throughout the total hours of a year (8760 h), the base hourly electric demand that should be met by the ORC would be 14.1 kWh. Consequently, a 15-kW ORC was selected for the model apartment building.

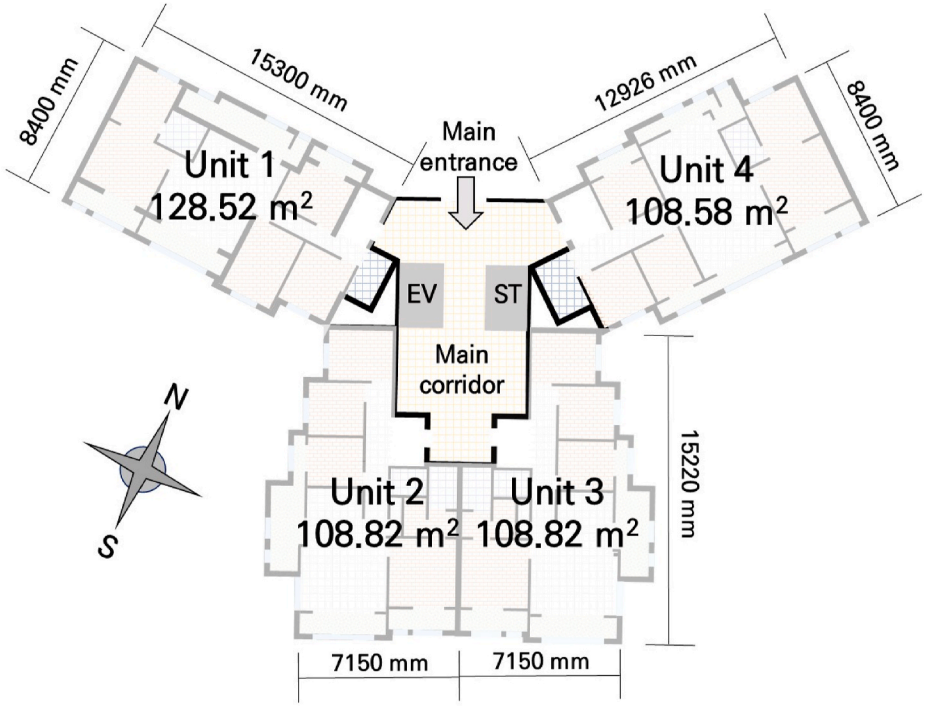

Fig. 3. Floor plan schematic of model building.

Table 2
Model building thermal-load information [36,37].

Location	Seoul, South Korea		
Occupants	4 people/unit		
Room setpoint	Winter 20 °C 30%	Intermediate season 24 °C 50%	Summer 26 °C 50%
Supply air setpoint	Heating mode 20 °C	Cooling mode 24 °C	
U-value	Outdoor wall 0.359 W/m^{2}K	Floor 0.352 W/m^{2}K	Window 1.12 W/m^{2}K
Internal heating element	Equipment 8 W/m^2	Light 2.7 W/m^2	Human body heat 75 W/person (sensible, latent)

4. Energy simulation

4.1. Component models of the proposed system

4.1.1. Absorber

The absorber efficiency in the LD system is expressed by Eq. (18). The humidity ratio of the air leaving from the absorber ($\omega_{ab,o}$) can be determined by using absorber efficiency (ε_{ab}) equation presented as an empirical model studied by Chung and Luo in the previous study (Eq. (19)) [39].

$$\varepsilon_{ab} = \frac{\omega_{ab,i} - \omega_{ab,o}}{\omega_{ab,i} - \omega_{ab,e}} \tag{18}$$

$$\varepsilon_{ab} = \left(1 - \frac{0.024\left(\frac{GFR_i}{LFR_i}\right)^{0.6} \exp\left(1.057\frac{DBT_{GFR_i}}{T_{LFR_i}}\right)}{(sZh)^{-0.185}\pi^{0.638}}\right) \Big/ \left(1 - \frac{0.192\exp\left(0.615\frac{DBT_{GFR_i}}{T_{LFR_i}}\right)}{\pi^{-21.498}}\right) \tag{19}$$

4.1.2. Regenerator

The regeneration efficiency can be expressed by Eq. (20). To determine the outlet humidity value of the regenerated air ($\omega_{reg,o}$), the regeneration efficiency (ε_{reg}) was predicted using Martin and Goswami's model [40] (Eq. (21)).

$$\varepsilon_{reg} = \frac{\omega_{reg,o} - \omega_{reg,i}}{\omega_{reg,e} - \omega_{reg,i}} \tag{20}$$

$$\varepsilon_{reg} = 1 - 48.3\left(\frac{L_i}{G_i}\right)^{\left(0.396\frac{\gamma_L}{\gamma_c} - 1.57\right)}\left(\frac{h_{oa,i}}{h_{sol,i}}\right)^{-0.751}(sZh)^{\left(0.0331\frac{\gamma_L}{\gamma_c} - 0.906\right)} \tag{21}$$

4.1.3. Chiller

The existing air-cooled chiller model [41] used in this work is shown in Appendix A. Eqs. (A.1) through (A.5) involve the following three performance curves: the capacity factor of cooling (A.2), input to output cooling energy factor (A.3), and partial-load efficiency of the chiller (A.4). The input parameters of CAPFT and EIRFT were the chilled water supply temperature (T_{CWS}) and the outdoor air temperature (T_{outa}).

4.1.4. Indirect evaporative cooler and reheating coil

The water pump energy consumed to supply the tap water on the wet channel of the indirect evaporative cooler is very small, thus is considered negligible. An electric heating coil was used for reheating the process air; the heating load of the coil was calculated using Eq. (22).

$$\dot{Q}_{reheat} = \dot{m}_a c_{p.a}\left(T_{sa} - T_{a.pro}\right) \tag{22}$$

4.2. Component models of reference systems

4.2.1. Desiccant wheel

The DW dehumidifies entering outdoor air and is regenerated by the exhaust air heated over 80 °C [42]. The latent effectiveness (Eq. (23)) and enthalpy effectiveness (Eq. (24)) should be known to determine the outlet air conditions.

$$\varepsilon_{RH} = \frac{RH_{pro.i} - RH_{pro.i}}{RH_{pro.i} - RH_{exh.i}} \tag{23}$$

$$\varepsilon_h = \frac{h_{pro.i} - h_{pro.i}}{h_{pro.i} - h_{exh.i}} \tag{24}$$

The energy calculation models of DW have been suggested in previous studies to predict the enthalpy effectiveness and relative humidity [42–44]. The empirical equations for the enthalpy and relative humidity effectiveness are described in Eqs. (A.6)–(A.11) and Eqs. (A.12)–(A.17), respectively. The velocities of the air were assumed to be 2 m/s at both sides of the DW. The wheel speed was set to 20 rph (0.33 rpm).

4.2.2. Gas-fired regeneration air heater

A gas-fired air heater was used as an auxiliary heat source for the regeneration. The exhaust air from the room was heated to 86 °C using a heating coil. The heater energy consumption for regeneration was estimated using Eq. (25) and involves the boiler efficiency curve (Eq. (27)), which is expressed as a function of part-load ratio (Eq. (26)) [41].

$$\dot{Q}_{heater} = \frac{\dot{Q}_{heating}}{Nominal\ thermal\ efficiency \times Boiler\ Efficiency\ Curve} \tag{25}$$

$$PLR = \frac{\dot{Q}_{heating}}{\dot{Q}_{heating,max}} \tag{26}$$

$$BEC = 0.626428326 + 0.645643582PLR - 0.77720685(PLR)^2 + 0.313806701(PLR)^3 \tag{27}$$

4.2.3. Enthalpy wheel

The EW was operated in the hot and humid outdoor air condition, and the EW rotates at 20 rpm when the maximum efficiency is shown. The efficiency of the EW is expressed by Eq. (28) [33]. The EW adjusts the target humidity ratio via rotating speed control according to Eqs. (A.18)–(A.25) when the maximum efficiency is not needed. Table B.1 presents the coefficients of the enthalpy speed control equations.

$$\varepsilon_{EW.h} = \frac{h_{pro.o} - h_{pro.i}}{h_{exh.i} - h_{pro.i}} \tag{28}$$

4.2.4. Sensible wheel

The SW exchanges the sensible heat with process air and exhaust air to satisfy the setpoint condition. The effectiveness of the SW expressed by Eq. (29) is assumed to be 80% at the full rotating speed (20 rpm)

$$\varepsilon_{SW} = \frac{DBT_{pro.i} - DBT_{pro.o}}{DBT_{pro.i} - T_{exh.i}} \tag{29}$$

4.2.5. Direct expansion coil

The DX-coil is used as an auxiliary dehumidifier or sensible cooler of the process air in the reference systems. The DX-coil energy consumption based on the air-cooled type was determined by the existing model expressed by Eqs. (A.26)–(A.36) in Appendix A [41].

4.3. Fan and pump

The fan power can be determined by using Equations (30) and (31). The designed total airflow rate ($\dot{V}_{tot.design}$) is calculated by the ventilation rate equation from Equation (15). The fan efficiency (η_{fan}) was set to be 50%. Appendix B provides the summary table of the pressure drop ($\sum \Delta P$) of each component (Table B.2). The pump power was determined by using Eq. (32). The design pump head (H) was assumed to be 15 m, and the pump efficiency (η_{pump}) was 60%.

$$P_{fan.design} = \frac{\dot{V}_{tot.design} \sum \Delta P}{\eta_{fan}} \tag{30}$$

$$P_{fan} = \left(0.0013 + 0.1470PLR_f + 0.9506PLR_f^2 + 0.0998PLR_f^3\right) \times P_{fan.design} \tag{31}$$

$$P_{pump} = \frac{\dot{V}_{fluid} gH}{\eta_{pump}} \tag{32}$$

5. Simulation results and discussions

5.1. Design-day performance

The main function of the three different centralized ventilation systems is dehumidifying the ventilation air to each unit of the model apartment building, while each system presents varying operating energy consumption. For understanding the energy consumption characteristics of each system for annual operation, energy simulation was initially performed for each system for the design day showing the highest humid ratio of the outside air because the ventilation systems should control the total latent load of the model building. If the ventilation system can dehumidify the highest humid air of the year, the dehumidification performance is reliable for all the year.

Fig. 4 demonstrates the air conditions of the outdoor and supply air on the design day. The design outdoor air condition was shown at 9:00 a.m. of the design day and pointed in Fig. 4.

The outdoor air conditioning process of the three systems is described on the psychrometric chart (Fig. 5) to evaluate the dehumidifying performance and, ultimately, the energy performance during the design day.

(1) Proposed system

In the proposed system described in Fig. 5(a), the incoming outdoor air at state P1 is dehumidified and the temperature is slightly decreased in the absorber of the LD system (i.e., at state P2). This is because the cold strong solution at least 25 °C is supplied to the

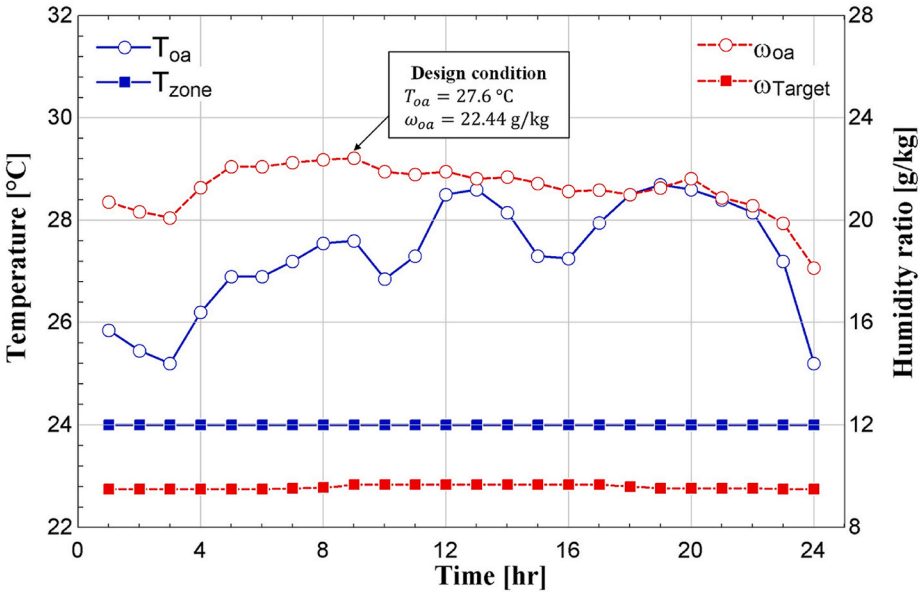

Fig. 4. Outdoor air and target supply air conditions on the design day.

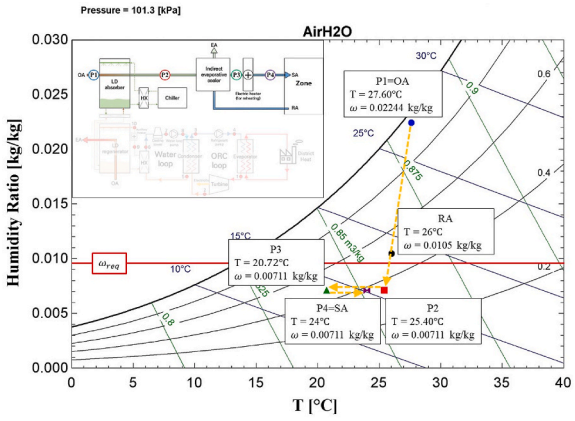

(a) Proposed system

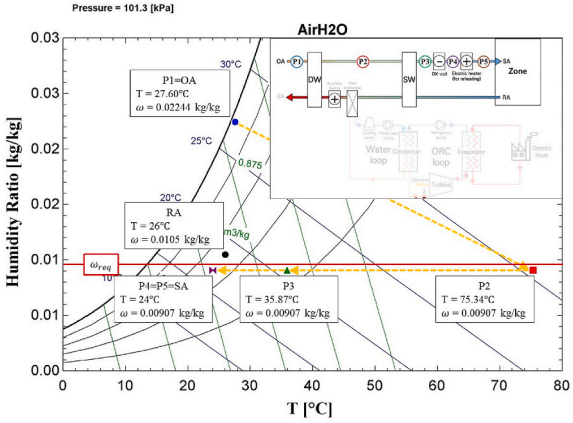

(b) Reference case 1 system

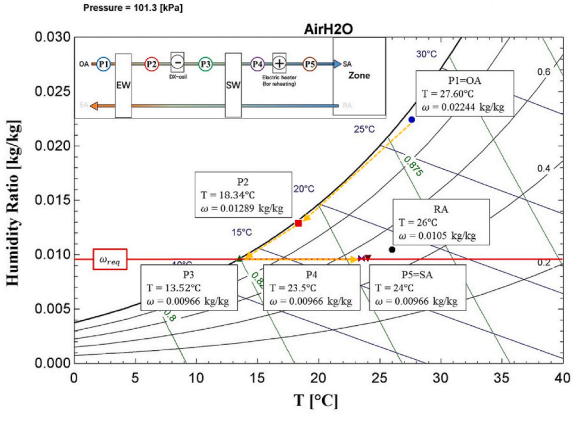

(c) Reference case 2 system

Fig. 5. Air conditioning process at the design condition.

absorber and solves this exothermic dehumidification process [45]. The remaining heat in the dehumidified process air is rejected by the indirect evaporative cooler. Thus, the air after the indirect evaporative cooler (i.e., at state P3) becomes 20.72 ° C of temperature and 0.00711 kg/kg of humidity ratio. The electric reheating coil is activated to reheat the leaving air from state P3 to meet the setpoint

temperature condition at state P4 (e.g., 24 ° C).

(2) Reference case 1 system

The air conditioning process of the reference case 1 was plotted in Fig. 5(b). The introduced air is initially dehumidified under the required humidity ratio line by the DW (at state P1). The hot and humid outdoor air at state P1 is heated up to 75.3 ° C at state P2 because the regeneration air is heated to 86 °C to regenerate the desiccant solution by using the ORC released heat. The SW is effectively utilized to reheat the process air by heat exchanging with conditioned zone air at state P3. The supply air setpoint temperature at state P4 (24 ° C) is met by the DX-coil. As the process air meets the supply condition through the DX-coil, the electric reheating coil does not operate and the air at state P5 is supplied to the conditioned zone under the same conditions as state P4.

(3) Reference case 2 system

The air conditioning process of the reference case 2 is presented in Fig. 5(c). The entering outdoor air at state P1 is cooled and dehumidified by the EW at state P2. The DX-coil should be activated to make the process air meeting the required humidity ratio of 0.00966 kg/kg (at state P3). The over-cooled dehumidified air is reheated by the SW using the sensible heat of the return air stream (at state P4). Additional heating of the process air would be required to supply air to each unit at the neutral temperature (at state P5).

5.2. System coefficient of performance

The latent load (i.e., dehumidification load) of the ventilation system is defined by Eq. (33) and the system COP is calculated by Eq. (34).

$$\dot{Q}_{dehum} = \dot{m}_{vent} h_{fg} (\omega_{oa} - \omega_{sa}) \tag{33}$$

$$COP_{system} = \frac{\dot{Q}_{dehum}}{\dot{W}_{chiller} + \dot{W}_{gas-fired\ heater} + \dot{W}_{electric\ heating\ coil} + \dot{W}_{DX-coil} + \dot{W}_{fan} + \dot{W}_{pump}} \tag{34}$$

As determined by Eq. (34), the highest system COP is the proposed system (i.e., 0.85–1.04) than reference cases 1 and 2 (i.e, 0.53–0.61 and 0.66–0.78, respectively) in the design day. The proposed system could show better energy performance because of the use of heat reclaimed from the ORC. The system COP of each system is also analyzed for the summer season. In Fig. 6, one can see that the proposed system is always operated with a higher COP than reference ventilation systems. The reference case 1 which is using the DW generally showed a nearly constant COP. However, the system shows a lower COP value than the proposed system because it consumes more energy compared to the amount of dehumidification. Meanwhile, the reference case 2 using the EW showed fluctuation of the system COP because of the EW exchanging enthalpy between outdoor air and indoor air. However, the proposed system showed higher COP than the reference case 2.

5.3. Energy consumption analysis

The result of the energy consumption converted in primary energy is presented for the design-day and annual operation in Figs. 7 and 8. The local primary energy factors [36] were applied in this study (i.e., 2.75 for electricity and 1.1 for natural gas). About

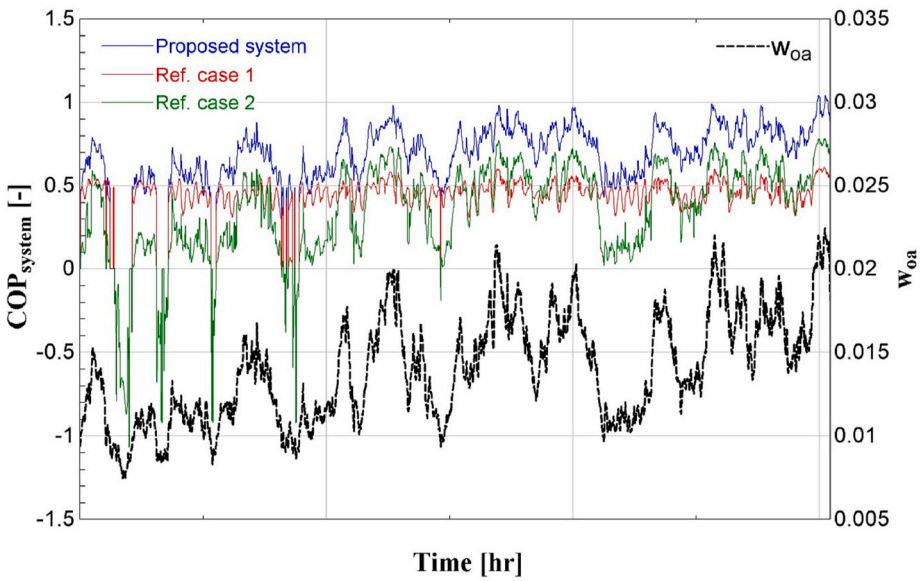

Fig. 6. System COP during the summer.

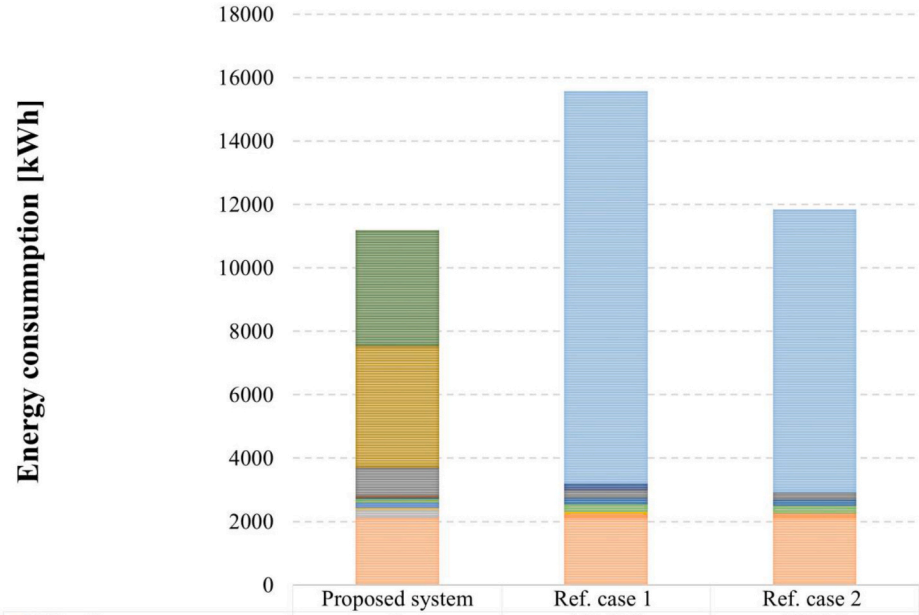

	Proposed system	Ref. case 1	Ref. case 2
DX-coil	0	12365.9	8932.8
Chiller	3647.1	0	0
Gas-fired heater (DW regen.)	0	201.6	0
Elec. HC (Aux. sol. heating)	3837.4	0	0
Elec. HC (Air reheating)	903.7	254.9	224.4
Fan (Regen.)	53.9	0	0
Fan (RA)	31.4	206.5	193.1
Fan (SA)	125.7	251.3	237.9
Pump (Solution circulation)	176.8	0	0
Pump (Water loop)	32.5	32.3	0
Pump (Chiller)	264.8	0	0
Pump (DX-coil)	0	135.3	143.8
Pump (ORC)	2.2	2.2	0
parallel heating	0	0	0
Parallel cooling	2113.8	2113.8	2113.8

Fig. 7. Comparison of system primary energy constumption on the design day.

design-day energy analysis (Fig. 7), The proposed system demonstrated 28% less primary energy in total energy consumption compared to that of reference case 1, and 6% less than that of reference case 2. The use of ORC released heat for the LD system in the proposed system and for the DW in reference case 1 was beneficial for reducing the purchased energy consumption for obtaining regeneration heat. However, since the DW used in reference case 1 should be regenerated to the high temperature, this can affect the increase of process air temperature leaving from the DW. Consequently, the reference case 1 consumed significant energy at the DX-coil for the satisfaction of the neutral air temperature condition (i.e., 24 ° C).

On the contrary, relatively less primary energy was consumed in the reference case 2 compared to that of the reference case 1 owing to efficient energy use in the DX-coil and heating the air for regeneration. However, the deep dehumidification by the DX-coil in reference case 2 presented an energy penalty compared to the proposed system, which is using the LD system. Therefore, the chiller energy performance is shown better than that of the DX-coil for dehumidifying the process air. Meanwhile, the same parallel cooling system for removing the sensible load of the target zone was considered in all three systems.

The energy analysis of each ventilation system was analyzed in an annual period. As one can see in Fig. 8(a), the annual ambient temperature profile is shown. The outdoor air condition ranges from a minimum of −13.8 ° C in winter to a maximum of 33.5° C in summer. The black dotted line shows the humidify trend line. One can see that the winter is relatively dry and the summer is in high humidity condition. Therefore, all three ventilation systems operate in dehumidification mode in summer and the dehumidifiers do not operate in other seasons. When annual operation simulations of all three systems were performed under these annual outdoor air conditions, the proposed system shows 24% and 4% less annual primary energy consumption than reference cases 1 and 2, respectively (Fig. 8(b)). The reference case 1 showed the highest annual primary energy consumption due to the significant energy penalty that occurred during the regeneration air heating and the DX-coil operation. The reference case 2 consumed more primary energy in the DX-coil for dehumidifying the process air than the proposed system.

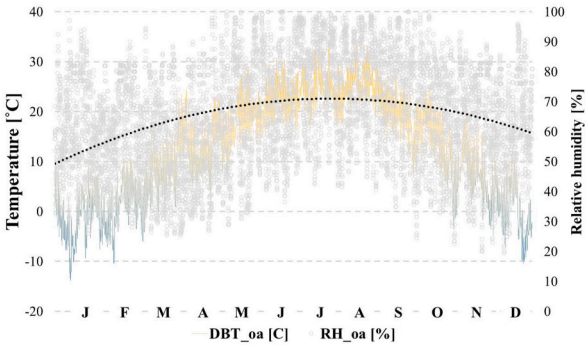

(a) Annual outdoor air condition.

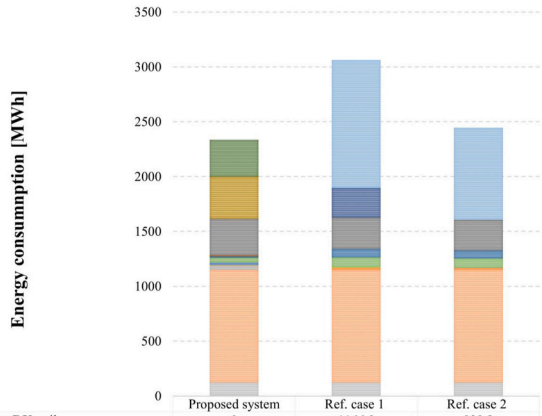

	Proposed system	Ref. case 1	Ref. case 2
DX-coil	0	1166.8	838.2
Chiller	336.6	0	0
Gas-fired heater (DW regen.)	0	270.2	0
Elec. HC (Aux. sol. heating)	385	0	0
Elec. HC (Air reheating)	333	286.8	280.2
Fan (Regen.)	7.4	0	0
Fan (RA)	11.6	76.7	71.8
Fan (SA)	46.5	93.2	88.3
Pump (Solution circulation)	24.5	0	0
Pump (Water loop)	4.4	4.4	0
Pump (Chiller)	35.2	0	0
Pump (DX-coil)	0	14.3	14.9
Pump (ORC)	0.3	0.3	0
Parallel cooling	1027	1027	1027
Parallel heating	123.3	123.3	123.3

(b) Annual primary energy consumption.

Fig. 8. Outdoor air conditions and comparison of system primary energy consumptions.

6. Conclusions

In this study, a central ventilation system was proposed for apartment buildings based on LD and evaporative cooling technologies integrated with the ORC, which generates electric power and heat from district heat. The energy benefit of the proposed system over two conventional dedicated outdoor air ventilation systems was demonstrated via detailed energy simulations. The proposed system presented better system COP (0.85–1.04) than reference system cases 1 and 2 which showed system COP of 0.53–0.61 and 0.66–0.78, respectively. The proposed system has 24% and 4% of the energy benefit in annual primary energy consumption less than reference cases 1 and 2, respectively. This is because using LD dehumidification integrated with the ORC and the evaporative cooling process is advantageous the energy saving in conditioning the ventilation air. Consequently, while the proposed system demonstrated sufficient energy-saving potential as a heat-driven centralized ventilation system, further experimental investigations should be performed to optimize the proposed system for practical use in residential buildings as a centralized ventilation system.

CRediT author statement

Beom-Jun Kim: Conceptualization, Methodology, Data curation, Writing original draft preparation. **Hye-Won Dong**: Methodology, Data curation, Validation. **Jae-Weon Jeong**: Supervision, Validation, Reviewing and Editing.

Declaration of competing interest

The authors declare that they have no known competing financial interests or personal relationships that could have appeared to influence the work reported in this paper.

Acknowledgments

This work was supported by the Korean Institute of Energy Technology Evaluation and Planning (KETEP) (No. 20202020800360).

Appendix A

(1) chiller (4.1.3.)

$$PLR = \frac{Q_{chiller}}{Q_{chiller.ref} CAPFT} \tag{A.1}$$

$$CAPFT = 0.9585465 + 0.0351687 T_{CWS} + 0.0001246624 T_{CWS}^2 - 0.002745559 T_{outa} - 0.000050002 32 T_{outa}^2 - 0.0001723494 T_{CWS} T_{outa} \tag{A.2}$$

$$EIRFT = 0.7327001 - 0.008343605 T_{CWS} + 0.0006385302 T_{CWS} - 0.003037535 T_{outa} + 0.0004849529 T_{outa} - 0.0008358498 T_{CWS} T_{outa} \tag{A.3}$$

$$EIRPLR = 0.04146742 + 0.6543795 PLR + 0.3044125 PLR^2 \tag{A.4}$$

$$P_{chiller} = P_{chiller.ref} \times CAPFT \times EIRFT \times EIRPLR \tag{A.5}$$

(2) Desiccant wheel (4.2.1.)

$$\varepsilon_{RH} = \alpha_{v,reg} \alpha_{v,pro} \alpha_{DBT} \alpha_{\omega} \alpha_N \tag{A.6}$$

$$\alpha_{v,reg} = -0.003286 v_{reg,i}^2 + 0.020519 v_{reg,i} + 0.095525 \tag{A.7}$$

$$\alpha_{v,pro} = 0.008343 v_{pro,i}^2 - 0.04322 v_{pro,i} + 0.16501 \tag{A.8}$$

$$\alpha_{DBT} = 1.1903 \ln\left(DBT_{reg,i} - DBT_{pro,i}\right) + 12.331 \tag{A.9}$$

$$\alpha_{\omega} = -4.519 \omega_{pro,i} + 0.80627 \omega_{reg,i} + 1 \tag{A.10}$$

$$\alpha_N = 0.0030464 r + 4.2846 \tag{A.11}$$

$$\varepsilon_h = \beta_{v,reg} \beta_{v,pro} \beta_{DBT} \beta_{\omega} \beta_N \tag{A.12}$$

$$\beta_{v,reg} = 0.22113 v_{reg,i}^{0.23493} \tag{A.13}$$

$$\beta_{v,pro} = 0.21763 v_{pro,i}^{-0.66335} \tag{A.14}$$

$$\beta_{DBT} = 0.00167789 DBT_{reg,i} - 0.0056224 DBT_{pro,i} + 1.671 \tag{A.15}$$

$$\beta_{\omega} = -44.505 \omega_{reg,i} + 27.728 \omega_{pro,i} + 1 \tag{A.16}$$

$$\beta_N = 0.13883 r + 4.6438 \tag{A.17}$$

(3) Enthalpy wheel (4.2.3.)

$$DFR = \frac{Q_{lat}}{Q_{sen}} \times \frac{1}{(RH_{outa}/100)^2} \cdot \left(when \cdot \dot{Q}_{sen} \le 0\right) \tag{A.18}$$

$$DFR = 2430.6 \times \frac{(w_{ra} - w_{outa})/(DBT_{ra} - DBT_{outa})}{(RH_{outa}/100)^2} \left(when \cdot \dot{Q}_{sen} > 0\right) \tag{A.19}$$

$$LE = 80 \cdot (\text{at full} - \text{speed operation mode}) \tag{A.20}$$

$$LE = \frac{HR_{sa.set} - HR_{outa}}{HR_{ra} - HR_{outa}} \times 100 \cdot (\text{at speed control mode}) \tag{A.21}$$

$$spd = c_1 + c_2(DFR) + c_3(DFR)^2 + c_4(LE) + c_5(LE)^2 + c_6(DFR)(LE) + c_7(DFR)^2(LE) + c_8(DFR)(LE)^2 + c_9(DFR)^2(LE)^2 \tag{A.22}$$

$$SE = 13.844 \times \ln(spd) + 38.469 \tag{A.23}$$

$$HR_{sa} = (LE / 100) \times (HR_{ra} - HR_{outa}) + HR_{outa} \tag{A.24}$$

$$DBT_{sa} = \left(\frac{SE}{100}\right) \times (DBT_{ra} - DBT_{outa}) + DBT_{outa} \tag{A.25}$$

(4) Direct expansion coil (4.2.5.)

$$ff = \frac{Actual\ air\ mass\ flow\ rate}{Rated\ air\ mass\ flow\ rate} \tag{A.26}$$

$$PLR = \frac{Required\ cooling\ load}{Capacity\ of\ chiller} \tag{A.27}$$

$$PLF = 0.85 + (0.15PLR) \tag{A.28}$$

$$RTF = \frac{PLR}{PLF} \tag{A.29}$$

$$TotCapTempModFac = 0.9600147 - 0.0106038WBT_{DX,i} + 0.0013516\left(WBT_{DX,i}\right)^2 + 0.0039357DBT_{outa,i} - 0.0000568\left(DBT_{outa,i}\right)^2 - 0.0004915\left(WBT_{DX,i}\right)\left(DBT_{outa,i}\right) \tag{A.30}$$

$$TotCapFlowModFac = 0.7491909 + 0.3721683ff - 0.1213592ff^2 \tag{A.31}$$

$$EIRTempModFac = 0.2484029 + 0.0610633WBT_{DX,i} - 0.0017081\left(WBT_{DX,i}\right)^2 + 0.0102658DBT_{outa,i} - 0.0007028\left(DBT_{outa,i}\right)^2 - 0.0004237\left(WBT_{DX,i}\right)\left(DBT_{outa,i}\right) \tag{A.32}$$

$$EIRFlowModFac = 1.2094575 - 0.3165036ff + 0.1070461ff^2 \tag{A.33}$$

$$Q_{cooling.DX} = 18.10122(TopCapTempModFac)(TotCapFlowModFac) \tag{A.34}$$

$$EIR = \left(\frac{1}{COP_{DX,rated}}\right)(EIRTempModFac)(EIRFlowModFac) \tag{A.35}$$

$$P_{DX} = Q_{cooling.DX}(EIR)(RTF) \tag{A.36}$$

Appendix B

Table B.1
Coefficients of the enthalpy wheel speed control equation [33].

LE	C1	C2	C3	C4
< 50%	2.344	−3.714	1.444	−0.005421
≥ 50%	−21.28	4.652	28.5	0.6905

(*continued on next page*)

Table B.1 (*continued*)

LE	C1	C2	C3	C4
C5	C6	C7	C8	C9
0.002286	0.05852	−0.0431	−0.001676	0.0006397
−0.00218	−0.4167	−0.8788	0.004481	0.006532

Table B.2
Fan pressure drop.

Components	Pressure drop (Δp)
LD absorber pad	120 Pa [46]
LD regenerator pad	120 Pa [46]
DW	150 Pa [44]
EW	120 Pa [47]
SW	100 Pa [48]
Indirect evaporative cooler	140 Pa [49]
SA duct balance	200 Pa
EA duct balance	200 Pa

References

[1] S. Quoilin, E. Systems, Sustainable Energy Conversion through the Use of Organic Rankine Cycles for Waste Heat Recovery and Solar Applications, Ph.D. Thesis, University of Liège, 2011, pp. 1–183, https://doi.org/10.1016/j.fsc.2004.06.001.

[2] B.F. Tchanche, G. Lambrinos, A. Frangoudakis, G. Papadakis, Low-grade heat conversion into power using organic Rankine cycles - a review of various applications, Renew. Sustain. Energy Rev. 15 (2011) 3963–3979, https://doi.org/10.1016/j.rser.2011.07.024.

[3] M. Kolahi, M. Yari, S.M.S. Mahmoudi, F. Mohammadkhani, Thermodynamic and economic performance improvement of ORCs through using zeotropic mixtures: case of waste heat recovery in an offshore platform, Case Stud. Therm. Eng. 8 (2016) 51–70, https://doi.org/10.1016/j.csite.2016.05.001.

[4] R. Kong, T. Deethayat, A. Asanakham, N. Vorayos, T. Kiatsiriroat, Thermodynamic performance analysis of a R245fa organic Rankine cycle (ORC) with different kinds of heat sources at evaporator, Case Stud. Therm. Eng. 13 (2019) 100385, https://doi.org/10.1016/j.csite.2018.100385.

[5] H. Wang, R. Peterson, T. Herron, Design study of configurations on system COP for a combined ORC (organic Rankine cycle) and VCC (vapor compression cycle), Energy 36 (2011) 4809–4820, https://doi.org/10.1016/j.energy.2011.05.015.

[6] H. Wang, R. Peterson, K. Harada, E. Miller, R. Ingram-Goble, L. Fisher, J. Yih, C. Ward, Performance of a combined organic Rankine cycle and vapor compression cycle for heat activated cooling, Energy 36 (2011) 447–458, https://doi.org/10.1016/j.energy.2010.10.020.

[7] X. Bu, L. Wang, H. Li, Performance analysis and working fluid selection for geothermal energy-powered organic Rankine-vapor compression air conditioning, Geoth. Energy 1 (2013) 1–14, https://doi.org/10.1186/2195-9706-1-2.

[8] H. Demir, M. Mobedi, S. Ülkü, A review on adsorption heat pump: problems and solutions, Renew. Sustain. Energy Rev. 12 (2008) 2381–2403, https://doi.org/10.1016/j.rser.2007.06.005.

[9] T. Katejanekarn, S. Kumar, Performance of a solar-regenerated liquid desiccant ventilation pre-conditioning system, Energy Build. 40 (2008) 1252–1267, https://doi.org/10.1016/j.enbuild.2007.11.005.

[10] F. Xiao, G. Ge, X. Niu, Control performance of a dedicated outdoor air system adopting liquid desiccant dehumidification, Appl. Energy 88 (2011) 143–149, https://doi.org/10.1016/j.apenergy.2010.06.019.

[11] S.J. Lee, H.J. Kim, H.W. Dong, J.W. Jeong, Energy saving assessment of a desiccant-enhanced evaporative cooling system in variable air volume applications, Appl. Therm. Eng. 117 (2017) 94–108, https://doi.org/10.1016/j.applthermaleng.2017.02.007.

[12] J. Lin, S.M. Huang, R. Wang, K.J. Chua, Thermodynamic analysis of a hybrid membrane liquid desiccant dehumidification and dew point evaporative cooling system, Energy Convers. Manag. 156 (2018) 440–458, https://doi.org/10.1016/j.enconman.2017.11.057.

[13] M.M. Rafique, P. Gandhidasan, H.M.S. Bahaidarah, Liquid desiccant materials and dehumidifiers - a review, Renew. Sustain. Energy Rev. 56 (2016) 179–195, https://doi.org/10.1016/j.rser.2015.11.061.

[14] S. Alizadeh, Performance of a solar liquid desiccant air conditioner - an experimental and theoretical approach, Sol. Energy 82 (2008) 563–572, https://doi.org/10.1016/j.solener.2007.10.009.

[15] K. Gommed, G. Grossman, A liquid desiccant system for solar cooling and dehumidification, J. Sol. Energy Eng. 126 (2004) 879, https://doi.org/10.1115/1.1690284.

[16] K. Gommed, G. Grossman, Experimental investigation of a liquid desiccant system for solar cooling and dehumidification, Sol. Energy 81 (2007) 131–138, https://doi.org/10.1016/j.solener.2006.05.006.

[17] M. Jradi, S. Riffat, Experimental investigation of a biomass-fueled micro-scale tri-generation system with an organic Rankine cycle and liquid desiccant cooling unit, Energy 71 (2014) 80–93, https://doi.org/10.1016/j.energy.2014.04.077.

[18] H.W. Dong, J.W. Jeong, Energy benefits of organic Rankine cycle in a liquid desiccant and evaporative cooling-assisted air conditioning system, Renew. Energy 147 (2020) 2358–2373, https://doi.org/10.1016/j.renene.2019.10.021.

[19] H.W. Dong, B.J. Kim, S.Y. Yoon, J.W. Jeong, Energy benefit of organic Rankine cycle in high-rise apartment building served by centralized liquid desiccant and evaporative cooling-assisted ventilation system, Sustain. Cities Soc. 60 (2020) 102280, https://doi.org/10.1016/j.scs.2020.102280.

[20] H. Ren, W. Gao, Y. Ruan, Optimal sizing for residential CHP system, Appl. Therm. Eng. 28 (2008) 514–523, https://doi.org/10.1016/j.applthermaleng.2007.05.001.

[21] O.A. Shaneb, G. Coates, P.C. Taylor, Sizing of residential μcHP systems, Energy Build. 43 (2011) 1991–2001, https://doi.org/10.1016/j.enbuild.2011.04.005.

[22] ASHRAE, ANSI/ASHRAE, Standard 62.2.-2016, Ventilation and Acceptable Indoor Air Quality in Low-Rise Residential Buildings, Refrigerating and Air-Conditioning Engineers, Inc., 2016.

[23] N. Fumo, D.Y. Goswami, Study of an aqueous lithium chloride desiccant system: air dehumidification and desiccant regeneration, Sol. Energy 72 (2002) 351–361, https://doi.org/10.1016/S0038-092X(02)00013-0.

[24] ASHRAE, ANSI/ASHRAE, District Heating Guide, American Society of Heating, Refrigerating and Air-conditioning Engineers, Inc., Atlanta, 2013.

[25] K. Yadav, A. Sircar, Selection of working fluid for low enthalpy heat source Organic Rankine Cycle in Dholera, Gujarat, India, Case Stud. Therm. Eng. 16 (2019) 100553, https://doi.org/10.1016/j.csite.2019.100553.

[26] S.I. Ata, A. Kahraman, R. Sahin, Prediction and sensitivity analysis under different performance indices of R1234ze ORC with Taguchi s multi-objective optimization, Case Stud. Therm. Eng. 22 (2020), https://doi.org/10.1016/j.csite.2020.100785.

[27] H.W. Dong, J.W. Jeong, Design and preliminary results of organic rankine cycle for liquid desiccant system, Appl. Therm. Eng. 178 (2020) 115596, https://doi.org/10.1016/j.applthermaleng.2020.115596.
[28] J. Bao, L. Zhao, A review of working fluid and expander selections for organic Rankine cycle, Renew. Sustain. Energy Rev. 24 (2013) 325–342, https://doi.org/10.1016/j.rser.2013.03.040.
[29] S. Quoilin, V. Lemort, J. Lebrun, Experimental study and modeling of an Organic Rankine Cycle using scroll expander, Appl. Energy 87 (2010) 1260–1268, https://doi.org/10.1016/j.apenergy.2009.06.026.
[30] H.W. Dong, J.W. Jeong, Energy benefits of organic Rankine cycle in a liquid desiccant and evaporative cooling-assisted air conditioning system, Renew. Energy 147 (2020) 2358–2373, https://doi.org/10.1016/j.renene.2019.10.021.
[31] M.H. Ahmed, N.M. Kattab, M. Fouad, Evaluation and optimization of solar desiccant wheel performance, Renew. Energy 30 (2005) 305–325, https://doi.org/10.1016/j.renene.2004.04.010.
[32] Y. Sheng, Y. Zhang, N. Deng, L. Fang, J. Nie, L. Ma, Experimental analysis on performance of high temperature heat pump and desiccant wheel system, Energy Build. 66 (2013) 505–513, https://doi.org/10.1016/j.enbuild.2013.07.058.
[33] J.W. Jeong, S.A. Mumma, W.P. Bahnfleth, Energy conservation benefits of a dedicated outdoor air system with parallel sensible cooling by ceiling radiant panels, ASHRAE Trans. 109 PART 2 (2003) 627–636.
[34] J.W. Jeong, Simplified Ceiling Radiant Cooling Panel and Enthalpy Wheel Models for Dedicated Outdoor Air System Design, 2004, pp. 1–201.
[35] ASHRAE, ASHRAE Handbook - Fundamentals, American Society of Heating, Refrigerating and Air-Conditioning Engineers, Inc., 2017.
[36] Korea Energy Agency, Energy Saving Design Standard of Buildings, Ministry of Land, Infrastructure and Transport, South Korea, 2018.
[37] ASHRAE, ANSI/ASHRAE, Standard 90.1-2016, Energy Standard for Buildings except Low-Rise Residential Buildings, Refrigerating and Air-Conditioning Engineers, Inc., 2016.
[38] I.Y. Choi, S.H. Cho, J.T. Kim, Energy consumption characteristics of high-rise apartment buildings according to building shape and mixed-use development, Energy Build. 46 (2012) 123–131, https://doi.org/10.1016/j.enbuild.2011.10.038.
[39] T.W. Chung, C.M. Luo, Vapor pressures of the aqueous desiccants, J. Chem. Eng. Data 44 (1999) 1024–1027, https://doi.org/10.1021/je990109q.
[40] V. Martin, D.Y. Goswami, Effectiveness of heat and mass transfer processes in a packed bed liquid desiccant dehumidifier/regenerator, HVAC R Res. 6 (2000) 21–39, https://doi.org/10.1080/10789669.2000.10391248.
[41] U.S. Department, Of Energy. Building Technologies Program, U.S. Department of Energy, Washington, DC, USA, 2013.
[42] S.Y. Cheon, H. Lim, J.W. Jeong, Applicability of thermoelectric heat pump in a dedicated outdoor air system, Energy 173 (2019) 244–262, https://doi.org/10.1016/j.energy.2019.02.012.
[43] S. De Antonellis, M. Intini, C.M. Joppolo, Desiccant wheels effectiveness parameters: correlations based on experimental data, Energy Build. 103 (2015) 296–306, https://doi.org/10.1016/j.enbuild.2015.06.041.
[44] NovelAire Technologies, Inc., 2021. https://www.novelaire.com/. (Accessed 21 January 2021).
[45] M.H. Kim, J.S. Park, J.W. Jeong, Energy saving potential of liquid desiccant in evaporative-cooling-assisted 100% outdoor air system, Energy 59 (2013) 726–736, https://doi.org/10.1016/j.energy.2013.07.018.
[46] A. Lowenstein, S. Slayzak, E. Kozubal, A Zero Carryover Liquid-Desiccant Air Conditioner for Solar Applications, Proceedings of 2006 ASME International Solar Energy Conference, American Society of Mechanical Engineers, 2006, pp. 397–407.
[47] S. De Antonellis, M. Intini, C.M. Joppolo, F. Pedranzini, Experimental analysis and practical effectiveness correlations of enthalpy wheels, Energy Build. 84 (2014) 316–323, https://doi.org/10.1016/j.enbuild.2014.08.001.
[48] S. De Antonellis, M. Intini, C.M. Joppolo, C. Leone, Design optimization of heat wheels for energy recovery in HVAC systems, Energies 7 (2014) 7348–7367, https://doi.org/10.3390/en7117348.
[49] ASHRAE, ASHRAE Handbook - HVAC Applications, American Society of Heating, Refrigerating and Air-Conditioning Engineers, Inc., 2020.